Large electronically mediated sputtering in gold films

Ajay Gupta*
Inter-University Consortium for DAE Facilities, University Campus, Khandwa Road, Indore 452001, India

D. K. Avasthi
Nuclear Science Center, P.O. Box 10502, Aruna Asaf Ali Marg, New Delhi 110067, India

(Received 31 July 2000; revised manuscript received 28 November 2000; published 27 September 2001)

Electronically mediated sputtering in thin gold films, bombarded with 200-MeV Ag ions, has been observed by *ex-situ* thickness measurements of the film using x-ray reflectivity technique. The observed sputter yield depends upon the film thickness and is about 410 atoms per incident ion for films of thickness 150 Å and 235 atoms per incident ion in 450-Å-thick film. This sputtering rate is a few orders of magnitude higher as compared to that normally encountered in the regime of elastic collisions. Reduced mobility of the electrons due to scattering from the surface and the grain boundaries plays an important role in enhancing the effects of electronic excitations. Sputtering is accompanied by a significant smoothening of the film surface and smearing of the boundaries between the grains.

DOI: 10.1103/PhysRevB.64.155407 PACS number(s): 79.20.−m, 61.80.Lj

Energetic heavy ions lose their energy in a medium by elastic collisions with the target nuclei as well as by inelastic collisions that results in the electronic excitation of the target atoms. At projectile energies greater than 100 keV/amu the dominant energy loss mechanism is electronic excitation and the rate of electronic energy loss $(dE/dx)_e$ lies typically in the range of 1–10 keV/Å. In insulators, the damage creation via such a high electronic excitation was demonstrated several decades back,[1] and more recently, electronically mediated sputtering has also been observed.[2–4] In metals, for a long time, such effects were considered to be unrealistic, as the high mobility of the conduction electrons would (i) very efficiently screen the ionized atoms, and (ii) quickly smear out the deposited energy. However, in recent years, sufficient evidence has been accumulated to show that, analogous to the case of insulators, electronic energy loss in metals can also create extensive atomic rearrangements;[5–11] creation of defects via electronic excitations, $(dE/dx)_e$, has been observed in many metals.[5,6] Latent tracks have also been observed above a certain threshold value of $(dE/dx)_e$ that varies from metal to metal.[7] Intermixing at metal-semiconductor and metal-metal interfaces using GeV heavy ions has also been reported.[8–11] In Fe/Si multilayers, the efficiency of mixing with 650 MeV/U ions has been found to be several orders of magnitude higher than that observed using ions of few 100 keV energies.[8] These studies suggest that electronic excitations should also induce surface-related processes, e.g., sputtering and morphological changes in metals. However, no direct observation of electronically mediated sputtering and associated changes in the surface morphology in metallic targets has been reported as yet. Studies on sputtering at high energies in gold foils have so far been performed by collecting the sputtered atoms in a catcher foil and analyzing this by Rutherford backscattering spectrometry.[12] The sputtering yield has been found to be about 9 Au atoms per incident 230-MeV Au ion. Numerous studies on swift heavy-ion-induced effects in metallic systems have demonstrated that in metallic thin films and multilayers, the effects of electronic energy loss are significantly enhanced, as compared to bulk materials.[8,10,13–15] In a series of works on ion-beam induced desorption of Au clusters on carbon backing, large desorption yields have been observed even for very low values of $(dE/dx)_e$.[13–15] Therefore, in the present work sputtering in Au thin films under the impact of 200-MeV Ag ions has been studied by x-ray reflectivity measurements. The associated changes in the surface morphology have also been studied using atomic force microscopy.

Thin films of high-purity gold (99.99%) were deposited on float-glass substrates in an ultrahigh vacuum of 1.0×10^{-9} mbar using electron-beam evaporation, with a deposition rate of 0.1 Å/s. Two sets of films with thicknesses of 150 and 450 Å were prepared. Films from both sets were bombarded with 200-MeV Ag ions to two different fluences of 1.0×10^{12} and 1.0×10^{13} ions/cm^2 using 15UD Pelletron at NSC, New Delhi. The ions were incident perpendicular to the Au films. The ion beam was scanned over an area of 1×1 cm^2. The ion current was kept at 0.1–0.2 particle nA ($1\ \text{pnA}=6.25\times10^9$ ions/s). The vacuum in the chamber during irradiation was $\sim10^{-7}$ mbar during irradiation.

The films were characterized using x-ray reflectivity, x-ray diffraction (XRD) and atomic-force-microscopy (AFM) measurements before and after irradiation. X-ray reflectivity and XRD measurements were done using Siemens

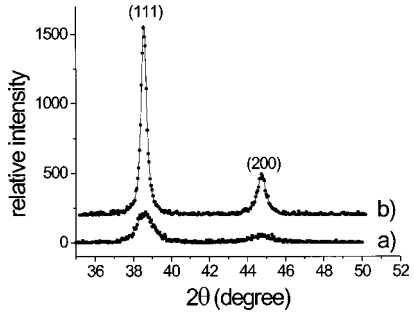

FIG. 1. X-ray diffraction pattern of the as-deposited Au films: (a) 150-Å-thick film, (b) 450-Å-thick film. The continuous curves represent theoretical fits to the data.

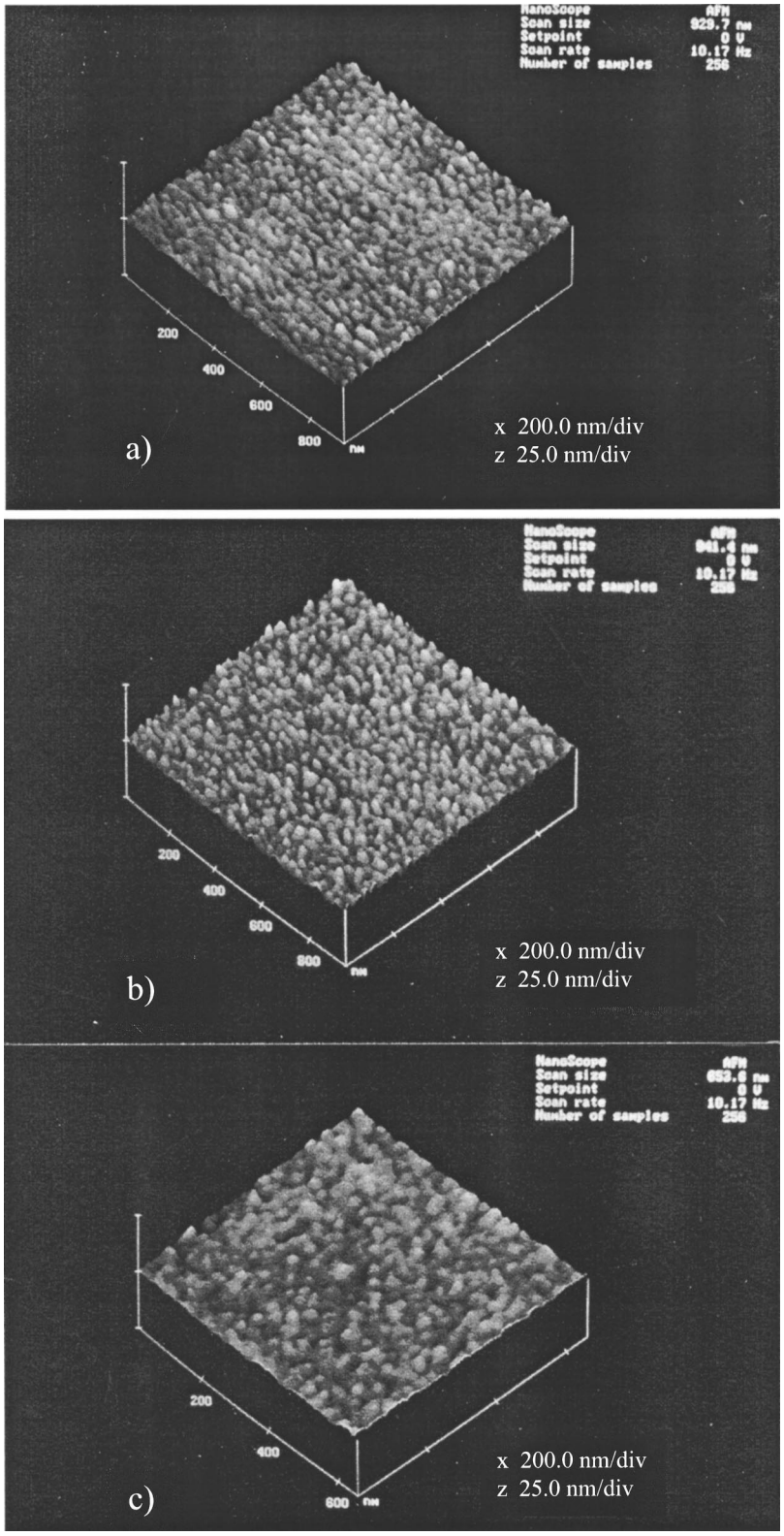

FIG. 2. AFM pictures of Au films: (a) 150-Å-thick film in as-deposited state, (b) 450-Å-thick film in as-deposited state, (c) 450-Å-thick film after irradiation with 200-MeV Ag ions to a fluence of 1.0×10^{13} ions/cm^2. Please note a different horizontal scale in the last picture.

*D*5000 diffractometer with Cu$K\alpha$ radiation. XRD measurements were done in an asymmetric Bragg-Brentano geometry with the angle of incidence kept at 0.5°. AFM measurements were done using Digital Nanoscope II.

Figure 1 gives the x-ray diffractograms of the two sets of films before irradiation. Both films have a texture along (111) direction. Average crystalline size along the scattering vector, obtained using Scherrer method, was 110 and 350 Å in films of thicknesses 150 and 450 Å, respectively. Irradiation did not have any observable effect on the XRD patterns of the films. Figures 2(a),(b) shows AFM pictures of the as-deposited films of thicknesses 150 and 450 Å. One may note

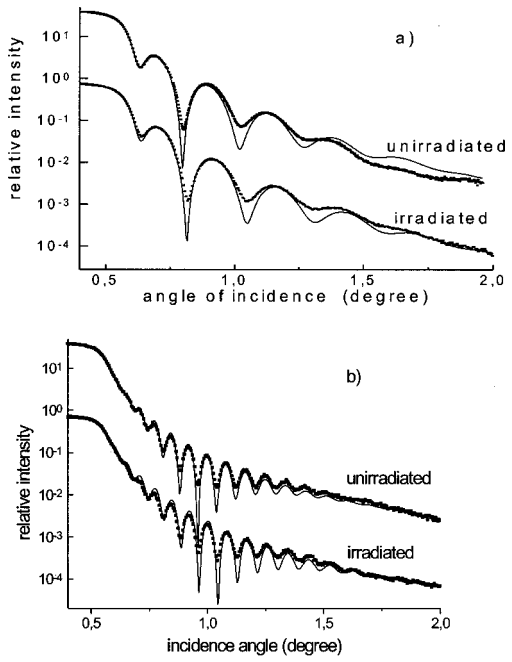

FIG. 3. X-ray specular reflectivity patterns of Au films before and after irradiation with 200-MeV Ag ions to a fluence of 1.0×10^{13} ions/cm^2: (a) 150-Å-thick film, (b) 450-Å-thick film. The continuous curves represent theoretical fits to the data. The reflectivity curves of unirradiated specimens are shifted upwards relative to the irradiated ones for the sake of clarity.

that both the films are continuous with rather uniform grain size. The average grain size in the film plane was estimated to be 350 Å in both the films.

Figure 3 gives the true specular x-ray reflectivity patterns of the two sets of the Au films before and after irradiation to a fluence of 1.0×10^{13} ions/cm^2. The amplitudes of the x rays specularly reflected from the two interfaces—air -to-gold and gold-to-glass—interfere with each other giving rise to "Kiessig oscillations,"[16] the period of which is determined by the thickness of the gold film through the modified Bragg equation

$$\sin\theta_n^2=\theta_c^2+(n+\tfrac{1}{2})^2\lambda^2/4t^2,$$

where θ_n is the angle for the maximum of the nth interference fringe, θ_c is the critical angle for total reflection, and t is the thickness of the film. The critical angle θ_c depends upon the refractive index of the gold film, which in turn depends upon its mass density. Experimentally obtained value of θ_c suggests that the mass density of the film is close to that of bulk Au and does not change after irradiation. High mass density of the film may be attributed to the fact that the deposition was done in an UHV environment with a very slow deposition rate. Reflectivity data was also computer fitted using the formalism of Parratt.[17] The thickness of the film and the average roughnesses of the two interfaces were taken as the fitting parameters. Refractive index $n=1-\delta-i\beta$ of the glass substrate was determined experimentally by fitting the reflectivity pattern of the substrate alone. The results of fitting are given in Table I.

From Table I one finds that within the experimental errors, the roughness of gold-to-glass interface remains unchanged even after the irradiation to a fluence of 1.0×10^{13} ions/cm^2. It may be noted that in a reflectivity pattern, the effect of a small intermixing at the interfaces is equivalent to that of an increased roughness (both lead to a less steep gradient of electron density across the interfaces). This suggests that the irradiation results neither in any intermixing at the gold-glass interface nor in any further roughening of glass surface. This second aspect was further checked independently by irradiating bare-float-glass substrates with 200-MeV Ag ions. X-ray reflectivity measurements show that roughness of the glass surface remains unchanged even after a fluence of 1.0×10^{13} ions/cm^2.

Perusal of Table I further shows that irradiation results in a reduction in the thickness of the films, the magnitude of which depends upon both the film thickness as well as the irradiation fluence. While irradiation to a fluence of 1.0×10^{12} ions/cm^2 does not lead to any detectable change in the thickness, a fluence of 1.0×10^{13} ions/cm^2 causes thickness reduction of 7 and 4 Å in specimens of thicknesses 150 and 450 Å, respectively. The corresponding sputtering rates come

TABLE I. Results of the fitting of x-ray specular reflectivity data of different films. t is the thickness of the layer, and σ is the rms roughness of the top interface of that layer. Subscripts 0 and i refer to the values of the parameters before and after irradiation. Roughness values as determined from XRR and AFM measurements are reported separately.

Designated Film thickness (Å)	Irradiation fluence (ions/cm^2)	Layer	t_0 (Å)	t_i (Å)	σ_0 (Å)		σ_i (Å)	
					XRR	AFM	XRR	AFM
150	10^{12}	Au	152±1	152±1	11.0±0.5	9.0±0.5	10.0±0.5	9.0±0.5
		Glass	∞	∞	3.5±1.0		3.5±1.0	
	10^{13}	Au	156	149	11.5	9.0	11.0	8.0
		Glass	∞	∞	4.0		4.0	
450	10^{12}	Au	455	455	14.0	11.5	13.0	9.0
		Glass	∞	∞	3.5		3.5	
	10^{13}	Au	454	450	14.0	11.5	12.5	8.0
		Glass	∞	∞	30		3.0	

out to be 410 and 235 atoms per incident Ag ion, respectively. Taking into account the uncertainities in the determination of the film thicknesses and the irradiation fluences, the uncertainty in the sputtering rate comes out to be ± 80 atoms per incident ion. TRIM calculations give the estimates for the electronic and nuclear energy losses by 200-MeV Ag ion in gold as 4.2 keV/Å and 16 eV/Å, respectively. Since the film thickness is small, the values of electronic energy loss and nuclear energy loss remain more or less uniform throughout the thickness of the film. The sputtering yield due to the nuclear collisions for the above value of $(dE/dx)_n$, as calculated using classical theory of Sigmund,[18,19] comes out to be only about 1.1 atom per incident ion. Thus, almost all of the observed yield is due to electronically mediated sputtering.

It may be noted that the sputtering yield per incident ion in the present case is a few orders of magnitude higher as compared to that normally encountered in the regime of the nuclear energy loss, and also as compared to that observed in some gold foils in the regime of electronic energy loss.[12] This large magnitude as well as film thickness dependence of the electronic sputtering rate can be understood in terms of the thermal spike model:[20] According to the thermal spike model, passage of the swift heavy-ion deposits a large amount of energy in the electronic system of the solid. Electron-electron interaction redistributes the energy within the electronic system leading to the thermalization of the energy. This occurs at a time scale of 10^{-15}–10^{-14} s. Electron-lattice interaction causes energy to transfer from electron system to lattice and thus inducing a lattice temperature increase at a time scale of 10^{-13}–10^{-12} s. Temperature of the thermal spike thus generated depends upon, (i) the volume in which the energy imparted by the swift ion diffuses due to the mobility of the hot electron gas, and (ii) the strength of electron-phonon coupling that determines the efficiency of the transfer of energy from electronic system to the lattice. Scattering of the excited electrons from the film surface, substrate-film interface, and also from the grain boundaries will reduce the mobility of the electrons as well as will increase the electron-phonon interaction. Further, in thin films density of structural defects is expected to be much higher as compared to the bulk material, which will further contribute to the reduction of electron mobility in films. Therefore, as compared to the bulk material, the temperature of the thermal spike is expected to be much higher in the case of thin films, thus enhancing the effects of electronic energy loss. Further, in the present case, AFM measurements show that the grain size in film plane is the same for both the films of thicknesses 150 and 450 Å. Therefore, a larger sputtering rate in the case of 150-Å-thick film is mainly due to increased scattering of the excited electrons from the film surface and interface.

Ion irradiation also causes observable changes in the surface morphology of the films. Perusal of AFM micrographs of as-prepared and irradiated specimens [Figs. 2(b),(c)] shows that the grain size remained unaffected by irradiation, however, a smearing of the grain boundary region is clearly visible after irradiation. Rms surface roughness σ was determined from the AFM scans on a frame of $1\times 1\ \mu m^2$ size. The average values of σ determined over five to eight frames for each specimen are also reported in Table I. Roughness measurements done using both x-ray reflectivity (XRR) and AFM show that irradiation results in smoothening of the film surface. Significant surface smoothening is observed even after an irradiation fluence of 10^{12} ions/cm^2. The glass-film interface is not significantly affected by irradiation. Smearing of the grain boundaries and associated decrease in the surface roughness suggests that the thermal spike is not limited to a single grain only, rather it spans a number of grains, thus resulting in atomic motion across the grain boundaries causing them to smear out.

In conclusion, an enhanced electronically mediated sputtering in Au film has been evidenced by direct measurement of the reduction in the film thickness using x-ray reflectivity measurement. Sputtering yield is more than two orders of magnitude higher than expected from elastic collision theory of Sigmund and is found to depend on the film thickness. The film-thickness dependence of the sputtering rate can be understood in terms of the thermal spike model, in which a reduced mobility of the electrons and a more efficient transfer of energy to the lattice due to scattering of the excited electrons from the surface and grain boundaries in the film results in an increased temperature of the thermal spike. Irradiation also results in a smearing of the grain boundaries and a significant smoothening of the film surface.

Thanks are due to Dr. V. Ganesan and Mr. P. Saravanan for help in doing the AFM measurements.

*Corresponding author. FAX: +91-731-465437. Email address: agupta@iucindore.ernet.in

[1] R. L. Fleischer, P. B. Brice, and R. M. Walker, J. Appl. Phys. **36**, 2645 (1965).

[2] G. Brinkmalm, P. Demirev, D. Fenyö, P. Hakansson, J. Kopniezky, and B. U. R. Sundqvist, Phys. Rev. B **47**, 7560 (1993).

[3] J. E. Griffith, R. A. Weller, L. E. Seiberling, and T. A. Tombrello, Radiat. Eff. **51**, 223 (1980).

[4] R. E. Johnson and W. L. Brown, Nucl. Instrum. Methods Phys. Res. **209/210**, 469 (1983).

[5] A. Iwase, S. Sasaki, and T. Nihira, Phys. Rev. Lett. **58**, 2450 (1987).

[6] A. Dunlop, D. Lesueur, P. Legrand, H. Dammak, and J. Dural, Nucl. Instrum. Methods Phys. Res. B **90**, 330 (1994).

[7] A. Barbu, A. Dunlop, D. Lesueur, and R. S. Averback, Europhys. Lett. **15**, 37 (1991); H. Dammak, A. Dunlop, D. Lesueur, A. Brunelle, S. Della Nagra, and Y. LeBeyee, Phys. Rev. Lett. **74**, 1135 (1995).

[8] C. Dufour, Ph. Bauer, G. Marchal, J. Grilhe, C. Jaouen, J. Pacaud, and J. C. Jousset, Europhys. Lett. **21**, 671 (1993); Ph. Bauer, C. Dufour, C. Jaouen, G. Marchal, J. Pacaud, J. Grilhe, and J. C. Jousset, J. Appl. Phys. **81**, 116 (1997).

[9] R. Leguay, A. Dunlop, F. Dunstater, N. Lorenzelli, A. Braslan, F. Bridon, J. Clrns, B. Padro, J. Chevallier, C. Coliese, A. Menelle, and J. L. Rouvire, Nucl. Instrum. Methods Phys. Res. B **106**, 28 (1996).

[10] Pratima Dhuri, Ajay Gupta, S. M. Chaudhari, D. M. Phase, and D. K. Avasthi, Nucl. Instrum. Methods Phys. Res. B **156**, 148 (1999).

[11] Ajay Gupta, Suneel Pandita, D. K. Awasthi, G. S. Lodha, and R. V. Nandedkar, Nucl. Instrum. Methods Phys. Res. B **146**, 265 (1998).

[12] H. D. Mieskes, W. Assmann, M. Brodale, M. Dobler, H. Glückler, and P. Hartung, Nucl. Instrum. Methods Phys. Res. B **146**, 162 (1998).

[13] K. L. Merkle, Phys. Rev. Lett. **9**, 157 (1962).

[14] H. H. Andersen, H. Knudsen, and P. Moller Petersen, J. Appl. Phys. **49**, 5638 (1978).

[15] I. Baranov, S. Jarmiychuk, S. Kirillov, A. Novikov, V. Obnorskii, A. Pchelintsev, K. Wien, and C. Reimann, Nucl. Instrum. Methods Phys. Res. B **157**, 167 (1999); I. Baranov, A. Novikov, V. Obnorskii, and C. T. Reimann, *ibid.* **146**, 154 (1998); I. Baranov, S. Bogdanov, A. Novikov, V. Obnorskii, and B. Kozlov, *ibid.* **122**, 329 (1997).

[16] T. C. Huang and W. Parrish, Adv. X-Ray Anal. **35**, 137 (1991).

[17] L. G. Parratt, Phys. Rev. **95**, 359 (1954).

[18] B. L. Hanke, E. M. Gullikson, and J. C. Devis, At. Data Nucl. Data Tables **54**, 181 (1993).

[19] P. Sigmund, Phys. Rev. **184**, 838 (1969).

[20] Z. G. Wang, Ch. Dufour, E. Paumier, and M. Toulemonde, J. Phys.: Condens. Matter **6**, 6733 (1994); **7**, 2525 (1995); M. Toulemonde, J. M. Costantini, Ch. Dufour, A. Meftah, E. Paumier, and F. Studer, Nucl. Instrum. Methods Phys. Res. B **116**, 37 (1996); T. Wiss, Hj. Matzke, C. Trautmann, M. Toulemonde, and S. Klaumunzer, *ibid.* **122**, 583 (1997); A. Meftah, M. Djebara, N. Khalfaoui, J. P. Stoquert, F. Studer, and M. Toulemonde, Mater. Sci. Forum **248–249**, 53 (1997).